Chapter 9

Macroscopic traffic flow models

Summary of chapter. The previous chapters of these notes discussed macroscopic traffic flow characteristics. It was show how the main variables density, flow and speed relate via the continuity equation and the conservation of vehicle equation. It was also discussed how these relations could be used to determine spatial-temporal dynamics of the traffic flow using shock wave analysis.

In this chapter, macroscopic traffic flow models are discussed. The aim of these models is to describe the dynamics of the traffic flow. Several macroscopic (or continuum) traffic flow models have proven to be simple enough for the real-time simulation of large traffic networks, while being sufficiently complex to realistically describe de principal aggregate traffic flow variables and their dynamics. These models are applicable due to the following reasons:

1. Macroscopic models describe the most important properties of traffic flows, such as the formation and dissipation of queues, shock waves, etc.

2. Macroscopic models are computationally less demanding. Moreover, the computational demand does not increase with increasing traffic densities, i.e. does not depend on the number of vehicles in the network.

3. They enable determination of average travel times, the mean fuel consumption and emissions in relation to traffic flow operations.

4. These models can be written in closed-form and are generally deterministic and less sensitive to small disturbances in the input.

In sum, macroscopic network traffic flow models are suitable for short-term forecasting in the context of network-wide coordinated traffic management. They are applicable in the development of dynamic traffic management and control systems, designed to optimise the traffic system and can be used to estimate and predict average traffic flow operations.

The underlying assumption of a macroscopic traffic flow model is that traffic can be described as a continuum, similar to a fluid or a gas. Macroscopic equations describing traffic flow dynamics are hence very similar to models for continuum media.

At this point, let us emphasise that the macroscopic models described in this section are in fact macroscopic in their representation of traffic. This does not necessarily imply that the traffic processes or the behaviour of the flow is described in aggregrate terms. On the contrary, several macroscopic models (i.e. the gas-kinetic models) consider the interaction between vehicles (or rather, the average number of interactions between the vehicles and the consequent average changes in the flow dynamics) explicitly. Although the representation of traffic is macroscopic, the behavioural rules describe the dynamics of the flow is in fact microscopic.

List of symbols

k	veh/m	traffic density
q	veh/s	traffic volume
$Q(k)$	veh/s	equilibrium flow as function of density
v	m/s	traffic speed
$V(k)$	m/s	equilibrium speed as function of density
ω	m/s	shock wave speed
c	m/s	kinematic wave speed
q_c	veh/s	capacity
r	veh/s	inflow (at on-ramp)
s	veh/s	outflow (at off-ramp)
$\tilde{N}(x,t)$	veh	cumulative vehicle count (smoothed)
$c(k), \lambda_*$	m/s	kinematic wave speed / characteristic speed
C	-	characteristics
$k_{i,j}$	veh/m	average density for $[x_{i-1}, x_i]$ at instant t_j
$q_{i,j}$	veh/s	average flow during $[t_j, t_{j+1}]$ at interface x_i
T_j	s	time step
l_i	m	cell length
D, S	veh/s	local demand, local supply
τ	s	relaxation time
$\lambda_{1,2}$	m/s	characteristic speeds for higer-order model
κ	veh/m	phase-space density
f	-	speed probability density function
V_0	m/s	desired (free) speed
π	-	immediate overtaking probability
σ	-	transition probability
Θ	m^2/s^2	speed variance

9.1 General traffic flow modelling issues

Traffic operations on roadways can be improved by field research and field experiments of real-life traffic flow. However, apart from the scientific problem of reproducing such experiments, the problem of costs and safety play a role of dominant importance as well. Traffic flow and micro-simulation models designed to characterise the behaviour of the complex traffic flow system have become an essential tool in traffic flow analysis and experimentation. Depending on the type of model, the application areas of these tools are very broad, e.g.:

- Evaluation of alternative treatments in (dynamic) traffic management.
- Design and testing of new transportation facilities (e.g. geometric designs).
- Operational flow models serving as a sub-module in other tools (e.g. traffic state estimation, model-based traffic control and optimisation, and dynamic traffic assignment).
- Training of traffic managers.

Research on the subject of traffic flow modelling started some forty years ago, when Lighthill and Whitham [34] presented a macroscopic modelling approach based on the analogy of vehicles in traffic flow with the dynamics of particles in a fluid. Since then, mathematical description of traffic flow has been a lively subject of research and debate for traffic engineers. This has resulted in a broad scope of models describing different aspects of traffic flow operations, such as microscopic and continuum (or macroscopic) models. The latter macroscopic (or rather

continuum models) consider the traffic flow as a continuum, i.e. like a fluid with specific characteristics, and are the topic of this chapter.

The description of observed phenomena in traffic flow is not self-evident. General mathematical models aimed at describing this behaviour using mathematical equations include the following approaches:

1. Purely deductive approaches whereby known accurate physical laws are applied.
2. Purely inductive approaches where available input/output data from real systems are used to fit generic mathematical structures (ARIMA models, polynomial approximations, neu-ral networks).
3. Intermediate approaches, whereby first basic mathematical model-structures are developed first, after which a specific structure is fitted using real data.

Papageorgiou [41] argues that it is unlikely that any microscopic or macroscopic traffic flow theory will reach the descriptive accuracy attained in other domains of science (e.g. Newtonian physics or thermodynamics). The author states that the only accurate physical law in traffic flow theory is the conservation of vehicles equation; all other model structures reflect either counter-intuitive idealisations or coarse approximations of empirical observations. Consequently, the challenge of traffic flow researchers is to look for useful theories of traffic flow that have sufficient descriptive power, where sufficiency depends on the application purpose of their theories.

9.2 Kinematic wave model and applications

As mentioned before, the most important equation in any macroscopic traffic flow model is the conservation of vehicle equation

$$\frac{\partial k}{\partial t} + \frac{\partial q}{\partial x} = r(x,t) - s(x,t) \tag{9.1}$$

where $k = k(x,t)$ denotes the traffic density, describing the mean number of vehicles per unit roadway length at instant t and location x; $q = q(x,t)$ denotes the traffic volume or flow rate, and describes the mean number of vehicles passing the cross-section x per unit time at time t; r and s respectively denote the inflow and outflow from and to on- and off-ramps.

The *kinematic wave model* (or LWR model, or first-order model) assumes that the traffic volume can be determined from the fundamental relation between the density and the traffic volume (or likewise, the speed), i.e.

$$q = Q(k) \tag{9.2}$$

In the previous chapter, we have illustation how, using shock wave theory, we can construct analytical solutions of the kinematic wave model for simple flow-density relations. However, it turns out that shock wave analysis will not predict the correct behaviour of the flow for any fundamental diagram, since it does not predict the occurence of so-called *acceleration fans* (described in the ensuing of this chapter). These acceleration fans describe the behaviour of traffic flowing out of a congested area, e.g. a queue of stopped vehicles.

9.2.1 Analytical solutions using method of characteristics

This section presents the so-called *method of characteristics* that can be applied to construct analytical solutions to the kinematic wave model. We can rewrite the conservation of vehicle equation (assuming that $r = s = 0$) as follows

$$\frac{\partial k}{\partial t} + Q'(k)\frac{\partial q}{\partial x} = 0 \tag{9.3}$$

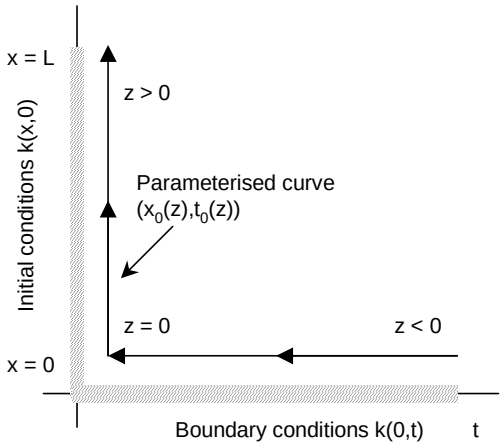

Figure 9.1: Parameterised curve $(x_0(z), t_0(z))$ describing the boundary of the region of interest.

where $Q'(k) = \frac{dQ}{dk}$. The kinematic wave model is a *first-order partial differential equation*. It is non-linear since $Q'(k)$ depends on k. The quantity $c(k) = Q'(k)$ will be referred to as the *characteristic speed*, since it describes the speed of the characteristic curves that play a pivotal role in the solution of hyperbolic equations, such as the kinematic model. For one, it turns out that the density k *is constant along any characteristic curve* of the kinematic wave model, and that the characteristic curves are therefore straight lines. It is also important to note that in the kinematic model the speed of the traffic $u(x,t)$ is always larger than the characteristic speed $c(k(x,t))$, i.e. traffic information never travels faster than the traffic that carries it. This implies that traffic flow is described as an *anisotropic fluid*: what happens behind a vehicle generally does not affect the behaviour of that vehicle.

Method of characteristics overview

Let us now take a closer look at solving equation (9.3). Let us first consider the boundary of the region of interest. Generally, the boundary consist of

1. the initial conditions (at $t = 0$) and
2. boundary conditions (at the start $x = 0$ and end $x = L$ of the roadway section).

We assume that we can construct a parameterised curve $(x_0(z), t_0(z))$ that describes these boundary of the region of interest. Fig. 9.1 shows an example of such a curve. Note that along this curve, the density is known!

For a specific value z, consider another parameterised curve C_z, starting from this boundary at location $(x_0(z), t_0(z))$

$$C_z = (x(s;z), t(s;z)) \quad \text{with} \quad x(0;z) = x_0(z) \quad \text{and} \quad t(0;z) = t_0(z) \tag{9.4}$$

For the example shown in Fig. 9.1, for $z > 0$, the curve C_z emanates from $t_0(z) = 0$ (the initial road conditions), while for $z < 0$, the curve emanates from $x_0(z) = 0$ (the upstream boundary of the region). We will define the curve by the following ordinary differential equations in t

$$\frac{dt}{ds} = 1 \quad \text{with} \quad t(0;z) = t_0(z) \tag{9.5}$$

$$\frac{dx}{ds} = c(k) = Q'(k) \quad \text{with} \quad x(0;z) = x_0(z) \tag{9.6}$$

for $s > 0$. Fig. 9.2 depicts two curves C_z, respectively emanating from the initial road conditions (in this case, for some $z > 0$) and from the boundary (for some $z < 0$). The curves C_z are

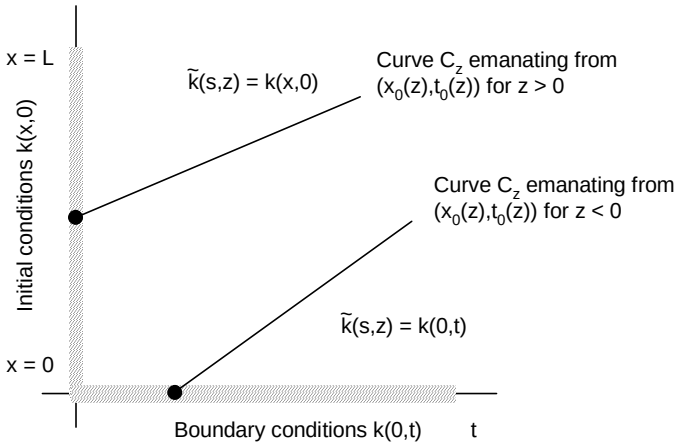

Figure 9.2: Curves C_z emanating from boundary describes by $(x_0(z), t_0(z))$.

called *characteristic curves* or *z-characteristics*.

By defining the curve C_z according to the equations (9.5) and (9.6), it turns out that the density $\tilde{k}(s;z) := k(x(s;z), t(s,z))$ along the curve C_z satisfies

$$\frac{d\tilde{k}}{ds} = \frac{\partial k}{\partial t}\frac{dt}{ds} + \frac{\partial k}{\partial x}\frac{dx}{ds} \tag{9.7}$$

$$= \frac{\partial k}{\partial t}\cdot 1 + \frac{\partial k}{\partial x}\cdot Q'(k) = 0 \tag{9.8}$$

Since $\frac{d\tilde{k}}{ds} = 0$, the density k along C_z is constant. More specifically, the density along C_z is equal to the density at the point where the curve C_z originates, i.e. at $s = 0$. As a result, we have

$$\tilde{k}(s;z) = k\left(x(s;z), t(s;z)\right) = k\left(x_0(z), t_0(z)\right) \tag{9.9}$$

Note that this implies that the curve C_z is a *straight line*, travelling at speed $\tilde{c}(z) = c\left(k\left(x(s;z), t(s;z)\right)\right)$.

To construct the solution of the kinetmatic wave model, initial and boundary conditions need to be established. By considering the curves emanating from the initial conditions as well as the boundaries, we can construct the solution $k(x,t)$ for $t > 0$ and $0 < x < L$.

If we, for the sake of argument, neglect the influence of the boundaries of the considered roadway section, we have seen that the formal solution of Eq. (9.3) is in fact

$$k\left(x + t\cdot ck(x,0), t\right) = k\left(x,0\right) \quad \text{for all } t > 0 \tag{9.10}$$

The speed of the characteristics (also referred to as *waves of constant density*) is equal to the derivative of the equilibrium flow $Q(k) = kV(k)$ and is hence positive as long as $k < k_c$ (unconstrained flow or free flow) and is negative as long as $k > k_c$ (constrained flow or congestion). Furthermore, the speed of the characteristics is bounded by the mean vehicle speed, i.e.

$$c(k) = \frac{dQ}{dk} = \frac{d\left(kV\left(k\right)\right)}{dk} = V(k) + k\frac{dV}{dk} < V(k) \tag{9.11}$$

since $\frac{dV}{dk} \leq 0$ (see Fig. 9.3). Only in the region when the average vehicle speed $V(k)$ is constant (the so-called *stable region*) and thus $\frac{dV}{dk} = 0$, we have $c(k) = V(k)$.

Effect of non-linearity of $Q\left(k\right)$

The objective of this section is to illustrate the effects of non-linearity of the flow-density curve, and particular the differences that will result when applying shock wave analysis and the LWR

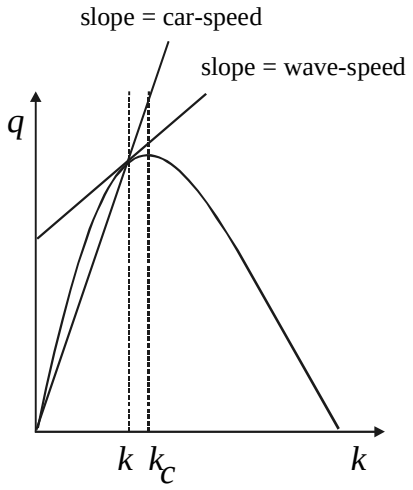

Figure 9.3: Interpretation of the wave speed

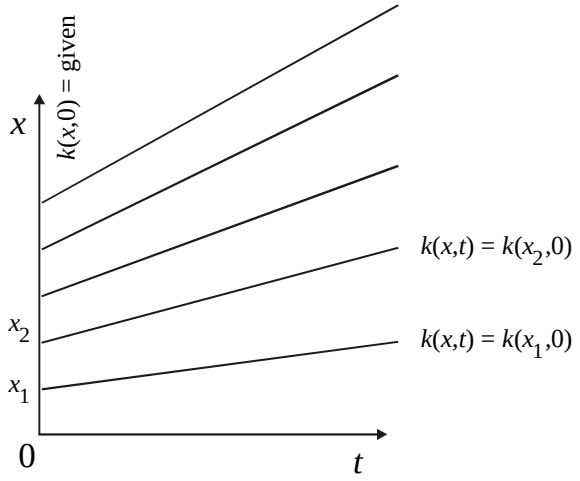

Figure 9.4: Lines of constant density

theory using non-linear flow-density curves. Waves of different density k will travel with different wave speeds $c(k) = Q'(k)$, and thus waves may either *fan out* or *converge and intersect*.

If $k(x,0)$ is a decreasing function of x (or equivalently, if the speed is an increasing function of x, so that cars are accelerating), then from Fig. 9.3 we notice that Q' - assumed to be a decreasing function of k - will be an increasing function of x. This corresponds to the situaiton illustrated in Fig. 9.4 in which the higher speed waves are initially ahead of the slower speed waves and so the region of acceleration tends to expand linearly with time as waves spread further and further apart. Fig. 9.5 shows a decreasing density $k(x,0)$ at time zero. A short time later the high density region has moved forward less than the low density region: a sharp initial change in density thus tends to disperse. At this point, we note that in this situation, we can determine the density $k(x,t)$ for all $t > 0$ is $k(x,0)$ is known. To this end, we only need to determine the slope of the characteristic emanating from $k(x,0)$ which intersects point (x,t), as s shown in Fig. 9.4.

If $k(x,0)$ is an *increasing function of* x, i.e. cars are decelerating, then the higher speed waves at low density are initially behind the slower speed waves for the higher density. A gradually increasing $k(x,0)$ tends to become steeper as shown in Fig. 9.6, and will eventually have a vertical tangent. This occurs as soon as any two waves of neighbouring values of k actually intersect. At this time, the solution (9.10) to the kinematic wave model breaks down

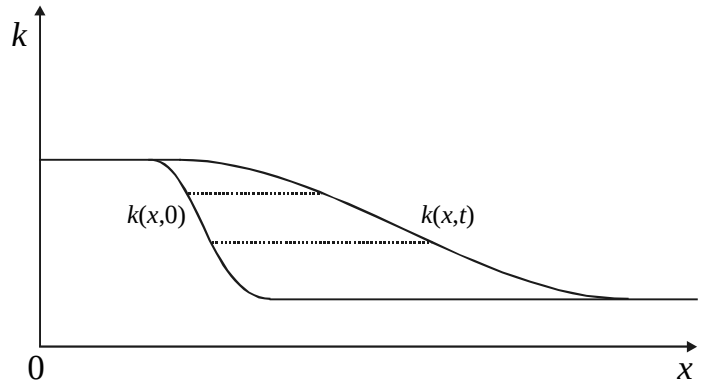

Figure 9.5: Dispersion of an acceleration wave

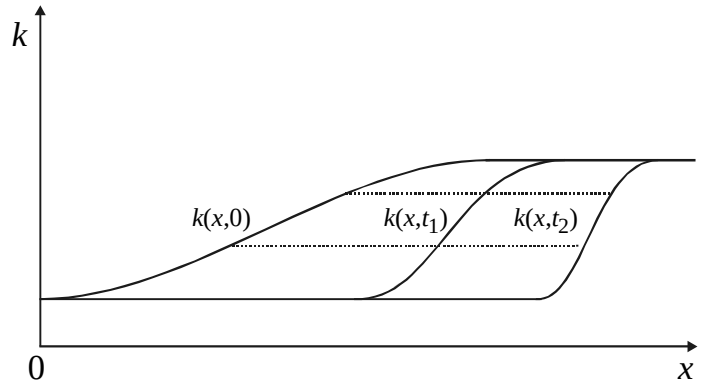

Figure 9.6: Focussing of deceleration waves

and , if it where continued beyond this time, would assign to some (x,t) point more than one value of k, becomes more than one wave passes through this point. The existence of a vertical tangent, however, means that $\frac{\partial k}{\partial x}$ becomes infinite and the differential equation from which the solution (9.10) was derived is no longer valid.

A phenomena such as this is familiar in fluid dynamics. The failure of the differential equation is corrected by allowing discontinuities in $k(x,t)$ which are called shocks. Shock wave theory was described in chapter 8 of these notes and is needed to complement the method of characteristics to find analytical solutions to kinematic wave model. In chapter 8 we have proven that the speed of the shock equals

$$\omega = \frac{q_2 - q_1}{k_2 - k_1} = \frac{Q(k_2) - Q(k_1)}{k_2 - k_1} \tag{9.12}$$

where k_1 and q_1 respectively denote the density and flow upstream of the shock S, and k_2 and q_2 denote the density and flow downstream of the shock. Recall that in the limit of very weak shocks, the shock line converges to the tangent of the Q curve (kinematic wave).

To evaluate $k(x,t)$, Eq. (9.12) is used to determine the path of the shock. Fig. 9.7 illustrates how in a typical problem one can construct the solution $k(x,t)$ graphically. If one is given $k(x,0)$ then one can draw the waves of constant k, or use the solution (9.10), to determine $k(x,t)$ at least until such time t_0 when two waves first intersect at a point (x_0,t_0). At this moment, a shock starts to form. Let us now determine the time t_0 and location x_0 at which this occurs.

Noe that except for very exceptional inital conditions $k(x,0)$ there is generally no *perfect focussing* of waves (waves converge on a single point). Therefore, the shock starts as an 'infinitesimal shock', meaning that the intersecting waves have nearly the same speed. The shock

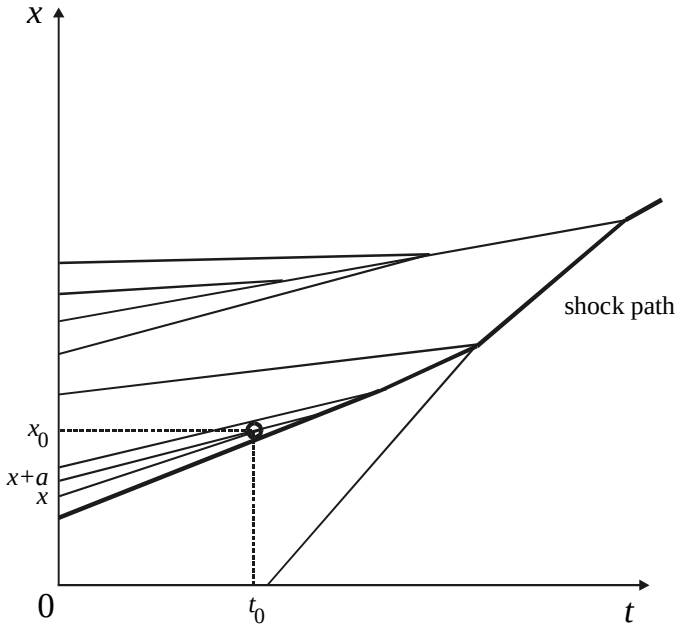

Figure 9.7: Construction of the shock path

will start with a speed approximately equal to those of the two intersecting waves. Futhermore, it is clear that the speed of the shock will have a speed which is between the speeds of the intersecting waves[1].

Let t_0 and x_0 be the first time two waves intersect and the location they intersection respectively. From Fig. 9.7 we observe that two waves starting at the points x and $x+a$ will intersect at this time t_0 and position x_0 given that the following condition is met:

$$x_0 = x + c(x)t_0 = x + a + c(x+a)t_0 \tag{9.13}$$

where $c(x) = Q'(k(x,0))$. Since t_0 is the first time any two waves intersect, it follows that

$$\frac{1}{t_0} = \max_{x,a} \frac{c(x) - c(x+a)}{a} \tag{9.14}$$

If $c(x)$ has a continuous derivative, it follows from the *mean value theorem* that $(c(x) - c(x+a))/a$ is equal to the derivate of c at some point between x and $x+a$. Therefore

$$\frac{1}{t_0} = \max_{x} \frac{dc}{dx} \tag{9.15}$$

The values of x for which the maximum is realised also give the values of x in Eqn. (9.13) that determine the position of x_0 where the shock originates.

We now know where the shock starts as well as its initial speed, thus also the position of the shock a short period later, at time $t_0 + \Delta t$. If no new shocks form between t_0 and $t_0 + \Delta t$, the values of k on either side of the shock at time $t_0 + \Delta t$ are still determined by the waves starting at $t = 0$. The density on either side of the shock is determined by the wave which intersects the schock at time $t_0 + \Delta t$ and approaches the shock from the same side. Another wave will approach from the other side and determine the density of that side. We now know the densities on either side of the shock at time $t_0 + \Delta t$ and we can reevaluate the shock speed at $t_0 + \Delta t$. We can then estimate the shock position at a still later time (e.g. $t_0 + 2\Delta t$), etc. In essesnce, we are performing a graphical integrtion of Eqn. (9.12).

[1] For weak shocks, the shock speed is approximately the average of the wave speeds at either side of the shock.

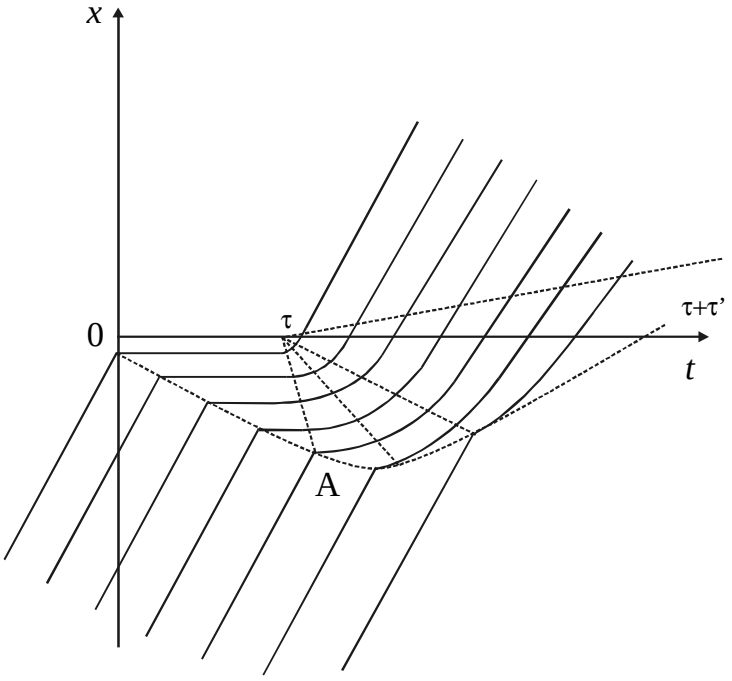

Figure 9.8: Cars stopped at a traffic signal

If some other shock should form elsewhere we proceed similarly to find their paths. If two shocks should intersect, we simple combine them into a single shock as shown in Fig. 9.7. The shock speed of the single shock is determined by the densities in the regions adjacent to the shock not including the region annihilated in the collision.

Example application of the kinematic wave model

As a practical example of how the kinematic wave model can be applied, let us consider what happens when a steady flow of traffic is suddenly stopped, for instance at an intersection, and then released again, as would occur at a traffic signal. The trajectories of cars which the theory should predict are shown in Fig. 9.8. The stopping point is at $x = 0$, and the trajectory of the first car that is stopped is designated by $x_1(t)$. The kinematic wave model *does not describe in detail the trajectory of car 1.* If we are given the density k_i, the intensity q_i or the speed v_i of the initial approach traffic strean, all other quantities are also determined by the $Q(k)$ relation. The speed at which car 1 approaches the stop line can be determined, since the traffic conditions are known. At the stopping line, the speed of the lead car is zero. The kinematic wave model does not describe the details of deceleration and acceleration of car 1, and additional information is required in order to correctly describe its behaviour. However, on a scale of time and distance in which the kinematic wave model aught to be applied, we may expect that deceleration and acceleration of car 1 is of negligible length of time.

The deceleration of the first car, being nearly instantaneous, creates a shock wave immediatly. It is a shock from the initial state (q_i, k_i) to the state $q = 0$ and $k = k_j$. The slope of the shock line in Fig. 9.9 between the states determines the shock speed. In Fig. 9.8, the shock starts at $x = 0$ and $t = 0$ and travels upstream with constant speed (shown by the dashed line). The shock line represents in effect the rear of the queue caused by the traffic signal. The continuum approximation implies that the decelerations occur practically instantaneously.

When the lead car accelerates again, it sends out a *fan of acceleration waves* for all car speeds between 0 and u_0. The slowest wave travels backwards with the wave speed c associatd with car speed $u = 0$. Clearly, this wave speed is given by the slope of $Q(k)$ at $k = k_j$, as shown in Fig. 9.9. When this wave starting at $x = 0$, $t = \tau$ as shown by the dashed line in Fig. 9.8

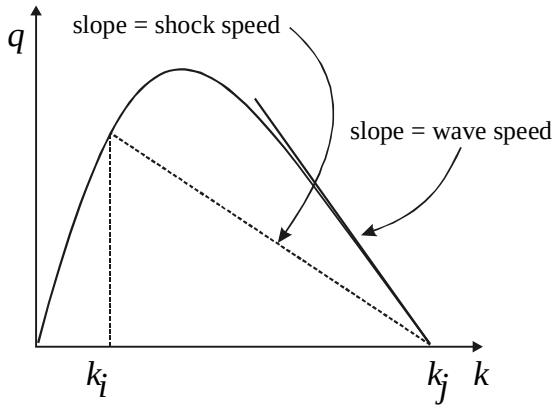

Figure 9.9: Evaluation of flows from a traffic signal

intersects the shock line at point A, this signals the car at the tail at the queue to move. The shock, however, does not apprear: the waves that intersect the shock only assign net values for the density or car speed on the front side of the shock. Since

$$\omega(t) = \frac{q_1 - q_2}{k_1 - k_2} = \frac{k_1 u_1 - k_2 u_2}{k_1 - k_2} \tag{9.16}$$

where ω again denotes the shock speed, and where state 1 and 2 respectively denote the state upstream and the state downstream of the shock. Since the flow q_1 upstream of the shock increases, the shock gains forward speed. It eventually moves with a positive speed and crosses the intersection at $x = 0$.

The time at which this occurs can be determined easily. We konw that the wave with the wave speed zero is the wave corresponding to q_c since the tangent to the $Q(k)$ curve is horizontal at $q = q_c$. The number of cars that cross the intersection before the shock arrives is therefore q_c multiplied by the time τ' for the shock to arrive. This must, however, also be equal to the total number of cars that have arrived by this time, i.e.

$$q_i(\tau + \tau') = q_c \tau' \tag{9.17}$$

in which τ is the length of time the traffic is stopped.

The shock, as it moves forward, becomes weaker and weaker. The car speeds at the rear of the shock remains at v_i but the car speeds at the front keep increasing. Eventually, the shock will overtake all waves for car speeds less thant v_i and the shock will degenerate into a wave or a shock of zero jump. The waves of car speeds larger than v_i however, move forward faster than te shock and the shock never reaches them.

9.2.2 Application of kinematic wave model for bicycle flows at signalised intersection

Consider a road on which a vehicle flow is moving in a certain direction. For the sake of argument, we assume that the flow is constant and equal to q_1. We assume that for the flow, the relation between density and flow can be approximated satisfactory using Greenshield's function

$$q\,(k) = u_0 k \left(1 - \frac{k}{k_j}\right) \tag{9.18}$$

where u_0 is the free speed of the vehicles and k_j is the jam-density. Assume that at the start of our analysis, no queue is present: traffic conditions are stationary and homogeneous (region 1). The density equals k_1 while the flow is equal to $q_1 = q\,(k_1)$. At a certain time (say, $t = -t_r$), the traffic signal that is present at $x = 0$ turns to red, causing the drivers to stop at the stopping

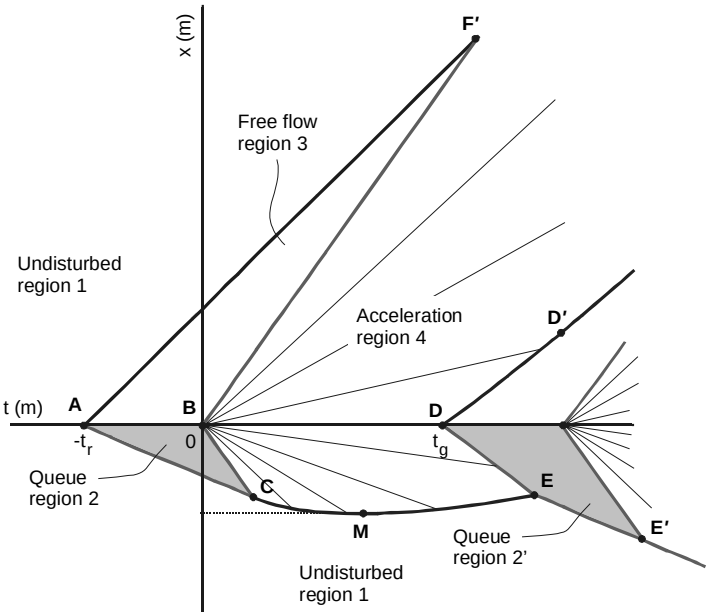

Figure 9.10: Emerging regions for controlled intersection example

line. Downstream of the stopping line, no vehicles will be present (region 3). As a result, a queue forms at the stopping line, which extend upstream (region 2, $x < 0$). At $t = 0$, the green phase starts and the first cyclists drive away from the stopping line. We assume that the drivers at the head of the queue react and accelerate instantaneously (without delay) *to the free speed* u_0. We have seen that the transition from the jam conditions for $x < 0$ to the free flow conditions downstream $x > 0$ causes a so-called *acceleration fan* (region 4). The acceleration fan described how the vehicles inside the congestion drive away from the queue.

At time $t = t_g$, the second red phase starts and cyclists are again held back at the stopping line. This causes the formation of a new queue (region $2'$). Fig. 9.10 shows qualitatively the predicted traffic flow conditions resulting when using the kinematic wave model. It also shows the different emerging regions as well as some points of interest. Furthermore, Fig. 9.11 shows a number of vehicle trajectories.

Let us now use what we have learnt so far to determine a mathematical solution to this problem. Let us first consider the shock wave between region 1 and region 2, described by the line $x_{AC}(t)$. The *speed of the shock wave cannot be determined from the method of characteristics.* Rather, we need to apply shock wave theory to determine the wave speed ω_{AC}. Since the traffic conditions upstream of the shock wave and downstream of the shock wave are constant, the shock speed is also constant. We find

$$\omega_{AC} = \frac{q_2 - q_1}{k_2 - k_1} = -\frac{q_1}{k_j - k_1} \tag{9.19}$$

which, by $(t_A, x_A) = (-t_r, 0)$

$$x_{AC}(t) = \omega_{AC} \cdot (t + t_r) = -\frac{q_1}{k_j - k_1}(t + t_r) \tag{9.20}$$

The next step is to determine the line $x_{AC}(t)$ describing the boundary between the jam region 2 and the acceleration region 4. The latter is described by the characteristics that are emanated from the point $(0, 0)$ (see Fig. 9.10). These characteristics are straight lines described by the kinematic wave speed

$$c(k) = q'(k) = u_0\left(1 - 2\frac{k}{k_j}\right) \tag{9.21}$$

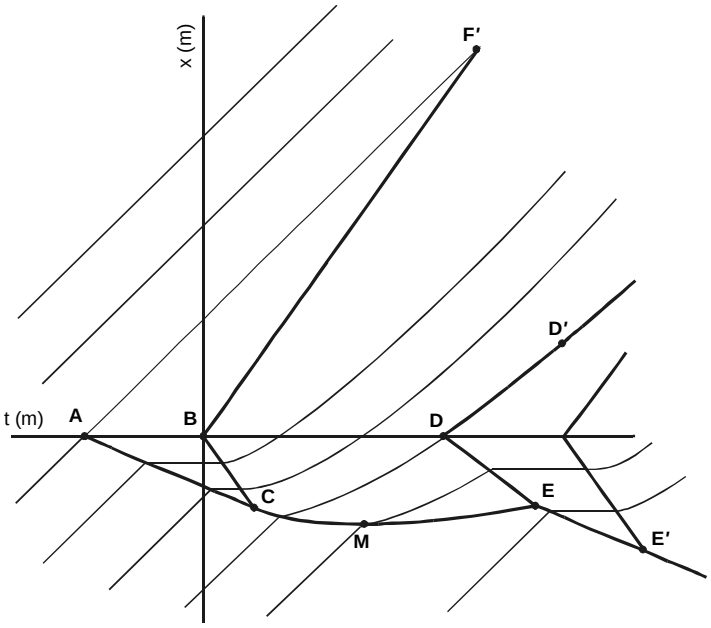

Figure 9.11: Example vehicle trajectories for controlled intersection example

The characteristic 'c' is then described by $x_c(t) = c \cdot t$, where $c \in [-u_0, u_0]$. It is very important to note that we can use this expression to determine the density $k_4(t,x)$ (and the speed and the flow) for all (t,x) in region 4:

$$k_4(t,x) = \frac{k_j}{2u_0}\left(u_0 - \frac{x}{t}\right) \tag{9.22}$$

$$u_4(t,x) = \frac{1}{2}\left(u_0 + \frac{x}{t}\right) \tag{9.23}$$

$$q_4(t,x) = \frac{1}{4}\frac{k_j}{u_0}\left[u_0^2 - \left(\frac{x}{t}\right)^2\right] \tag{9.24}$$

for all (t,x) in region 4.

The characteristic that moves *upstream* (in the direction $x < 0$) at the highest speed moves upstream with speed $-u_0$. This is precisely the characteristic that separates region 2 and region 4. Thus, the line $x_{BC}(t)$ moves with speed $-u_0$ and is thus given by the following expression (since $x_{BC}(0) = 0$)

$$x_{BC}(t) = -u_0 t \tag{9.25}$$

We can then determine the coordinates of point C easily. Some straightforward computations show that

$$t_C = \frac{k_1}{k_j - k_1} t_r \quad \text{and} \quad x_C = -u_0 t_C = -u_0 \frac{k_1}{k_j - k_1} \tag{9.26}$$

The next step is to determine a relation for the shock wave $x_{CE}(t)$ separating undisturbed region 1 and the acceleration region 4. On the contrary to the shock wave $x_{AC}(t)$, the speed of the shock $x_{CE}(t)$ is *not constant* since the downstream conditions (in region 4) are non-stationary (since they satisfy Eqns.(9.22)-(9.23)). We can still however apply shock wave theory on the non-stationary conditions. This provides us with the following expression for the shock wave speed $\omega_{CE}(t)$ describing the slope of line $x_{CE}(t)$

$$\omega_{CE}(t) = \frac{q_4 - q_1}{k_4 - k_1} = \frac{1}{2}\frac{k_j\left[u_0^2 - \left(\frac{x_{CE}(t)}{t}\right)^2\right] - 4q_1u_0}{k_j\left[u_0 - \left(\frac{x_{CE}(t)}{t}\right)\right] - 2k_1u_0} \tag{9.27}$$

Since

$$x_{CE}(t) = x_{CE}(t_C) + \int_{t_C}^{t} \omega_{CE}(s)\, ds \tag{9.28}$$

we can determine $x_{CE}(t)$ by solving the following ordinary differential equation

$$\frac{d}{dt} x_{CE} = \omega_{CE}(t) \quad \text{with} \quad x_{CE}(t_C) = x_C \tag{9.29}$$

where $\omega_{CE}(t)$ depends on $x_{CE}(t)$ according to Eq. (9.27). Solving this differential equation is not straightforward and requires application of the method of *variation of constants*. We can determine that:

$$x_{CE}(t) = c(k_1)\, t - (u_0 + c(k_1)) \sqrt{t_C t} \tag{9.30}$$

is the solution that satisfies Eq. (9.29).

Proof. Consider the ordinary differential equation

$$\frac{dx}{dt} = \frac{1}{2} \frac{k_j \left[u_0^2 - \left(\frac{x}{t}\right)^2\right] - 4 q_1 u_0}{k_j \left[u_0 - \left(\frac{x}{t}\right)\right] - 2 k_1 u_0} \tag{9.31}$$

Define $x = ty$. Then

$$\frac{dx}{dt} = t \frac{dy}{dt} + y \tag{9.32}$$

and thus Eq. (9.31) becomes

$$t \frac{dy}{dt} + y = \frac{1}{2} \frac{k_j \left(u_0^2 - y^2\right) - 4 q_1 u_0}{k_j (u_0 - y) - 2 k_1 u_0} \tag{9.33}$$

Then, we can easily derive that

$$t \frac{dy}{dt} = \frac{k_j \left(u_0^2 - y^2\right) - 4 q_1 u_0 - 2 k_j (u_0 - y)\, y + 4 k_1 u_0 y}{2 k_j (u_0 - y) - 4 k_1 u_0} \tag{9.34}$$

$$= k_j \frac{y^2 - 2 u_0 \left(1 - 2\frac{k_1}{kj}\right) y + u_0^2 - 4 \frac{q_1}{k_j} u_0}{2 k_j (u_0 - y) - 4 k_1 u_0} \tag{9.35}$$

$$= \frac{1}{2} \frac{y^2 - 2 u_0 \left(1 - 2\frac{k_1}{kj}\right) y + u_0^2 - 4 \frac{k_1 u_0 \left(1 - \frac{k_1}{k_j}\right)}{k_j} u_0}{u_0 \left(1 - 2\frac{k_1}{k_j}\right) - y} \tag{9.36}$$

$$= \frac{1}{2} \frac{y^2 - 2 u_0 \left(1 - 2\frac{k_1}{kj}\right) y + u_0^2 \left(1 - 2\frac{k_1}{k_j}\right)^2}{u_0 \left(1 - 2\frac{k_1}{k_j}\right) - y} \tag{9.37}$$

Note that $c(k_1) = u_0 \left(1 - 2\frac{k_1}{k_j}\right)$ and $c^2(k_1) = u_0^2 \left(1 - 2\frac{k_1}{k_j}\right)^2$ and thus

$$t \frac{dy}{dt} = -\frac{1}{2} \frac{y^2 - c(k_1)\, y + c^2(k_1)}{y - c(k_1)} = -\frac{1}{2} \frac{(y - c(k_1))^2}{y - c(k_1)} = -\frac{1}{2} y + \frac{1}{2} c(k_1) \tag{9.38}$$

We can again use Eq. (9.32) to see that the equation above becomes

$$t \frac{dy}{dt} + y - \frac{1}{2} y = \frac{1}{2} c(k_1) \rightarrow \frac{dx}{dt} = \frac{1}{2} \frac{x}{t} + \frac{1}{2} c(k_1) \tag{9.39}$$

This is a linear differential equation, which can be solved by variation of constants. To this end, we first determine the solution to the reduced differential equation

$$\frac{dx}{dt} = \frac{1}{2} \frac{x}{t} \tag{9.40}$$

which equals

$$x = C\sqrt{t} \tag{9.41}$$

The variation of constant approach involves trying the following solution in the non-reduced differential equation (9.39)

$$x = C(t)\sqrt{t} \tag{9.42}$$

which yields

$$\frac{dx}{dt} = C(t)\frac{1}{2}\frac{1}{\sqrt{t}} + \frac{dC}{dt}\sqrt{t} = \frac{1}{2}\frac{C(t)}{\sqrt{t}} + \frac{1}{2}c(k_1) \tag{9.43}$$

$$\frac{dC}{dt}\sqrt{t} = \frac{1}{2}c(k_1) \tag{9.44}$$

and thus $C(t) = c(k_1)\sqrt{t} + C_0$, which in turn yields

$$x(t) = \left(c(k_1)\, t + C_0\sqrt{t}\right) \tag{9.45}$$

We can determine the integration constant C_0 by using the boundary condition $x(t_C) = x_C$

$$C_0 = -\left(u_0 + c(k_1)\right)\sqrt{t_C} \rightarrow x(t) = c(k_1)\, t - \left(u_0 + c(k_1)\right)\sqrt{t_C t} \tag{9.46}$$

■

Let us assume that the next red phase starts at $t = t_g$ before the shock x_{CE} has reached the stopping line. Let us first describe the shock wave between region 4 and region $3'$. Again, this shock will not move at a constant speed, since the traffic conditions upstream of the shock are non-stationary. We have

$$\omega_{DD'}(t) = \frac{q_4 - q_{3'}}{k_4 - k_{3'}} = \frac{q_4}{k_4} = u_4 \tag{9.47}$$

that is, the speed of the shock equals the speed of the last vehicle emanating from the queue before the start of the second red phase. Again we need to solve a differential equation to determine the shock wave $x_{DD'}(t)$

$$\frac{d}{dt}x_{DD'} = \frac{1}{2}\left(u_0 + \frac{x_{DD'}}{t}\right) \quad \text{with} \quad x_{DD'}(t_g) = 0 \tag{9.48}$$

which results in

$$x_{DD'}(t) = u_0\left(t - \sqrt{t \cdot t_g}\right) \tag{9.49}$$

Proof. Eq. (9.48) is an ordinary linear differential equation of the general form $a(t)\frac{dx}{dt} = b(t)\, x + c(t)$. To solve differential equations of this sort, we first consider the reduced differential equation

$$\frac{dx}{dt} = \frac{x}{2t} \tag{9.50}$$

which is easily solved by separating the variables x and t

$$\frac{1}{x}dx = \frac{1}{2t}dt \tag{9.51}$$

which is solved by

$$\ln x = \frac{1}{2}\ln x + C \tag{9.52}$$

for some integration constant C; x thus satisfies

$$x = C\sqrt{t} \tag{9.53}$$

To solve the non-reduced differential equation, the *variation of constant* method is used. That is, we try the following solution

$$x = C(t)\sqrt{t} \tag{9.54}$$

Substituting this solution in Eq. (9.48) yields

$$C(t) = u_0\sqrt{t} + C_0 \tag{9.55}$$

The integration constant C_0 can be determined by considering the initial condition $x(t_g) = 0$ which yields the solution

$$x(t) = u_0\left(t - \sqrt{t \cdot t_g}\right) \tag{9.56}$$

■

In a similar way, we can determine the shock wave $x_{DE}(t)$ separating region 4 and region $2'$. The speed of the shock wave equals

$$\begin{aligned} \omega_{DE}(t) &= \frac{q_{2'} - q_4}{k_{2'} - k_4} = -\frac{q_4}{k_j - k_4} && (9.57)\\ &= -\frac{1}{2}\left[u_0 - \left(\frac{x_{DE}}{t}\right)\right] && (9.58) \end{aligned}$$

and thus

$$\frac{d}{dt}x_{DE} = -\frac{1}{2}\left[u_0 - \left(\frac{x_{DE}}{t}\right)\right] \quad \text{with} \quad x_{DE}(t_g) = 0 \tag{9.59}$$

which has the following solution

$$x_{DE}(t) = -u_0\left(t - \sqrt{t_g t}\right) \tag{9.60}$$

Finally, the shock $x_{EE'}(t)$ separating region 1 and region $2'$ moves at constant speed $\omega_{EE'}$ which equals

$$\omega_{EE'} = \omega_{AC} \tag{9.61}$$

9.2.3 Implications for fundamental diagram

The previous section showed how the method of characteristics can be applied to determine solutions to the kinematic wave model. We have seen how shocks are formed in regions where the speed decreases with space. We have also seen how traffic leaving a queue gives rise to a so-called *acceleration fan*, consisting of characteristics with different speeds $c(k) = \frac{d}{dk}Q(k)$.

Implicitly, during the analysis, we have used special assumptions regarding the shape of the fundamental diagram. More precisely, we assumed that the fundamental diagram $Q(k)$ is a *concave function*, i.e.

$$\frac{d^2Q}{dk^2} \leq 0 \tag{9.62}$$

Let us illustrate why this property is important to represent traffic behaviour correctly. To this end, consider a flow-density curve that is non-concave in the congested branch. Consider the case illustrated by Fig. 9.13. In this case, the initial conditons $k(x,0)$ describe the case of smoothly decreasing densities. Note that when the $Q(k)$ function is concave, this region would smooth out further. Fig. 9.13 shows that, since the congested branch of $Q(k)$ is convex instead of concave, the slopes of the characteristics emanating from the initial conditions at $t = 0$ become more negative as x increases. In the end, the waves even intersect, causing a shock wave. In other words, although dense traffic travels slower, the waves the dense traffic carries travel faster than the waves in light traffic, given rise to the shock. This shock is thus formed by traffic that drives out of the high into the lower density region.

Exercise 55 *Describe yourself what will happen in the convex region of the fundamental diagram in case the initial $k(x,0)$ describes conditions in which the density $k(x,0)$ increases with increasing x. Also discuss why this is not realistic.*

Remark 56 *Appendix A discusses an alternative solution approach for the kinematic wave model that is based on application of Green's theorem.*

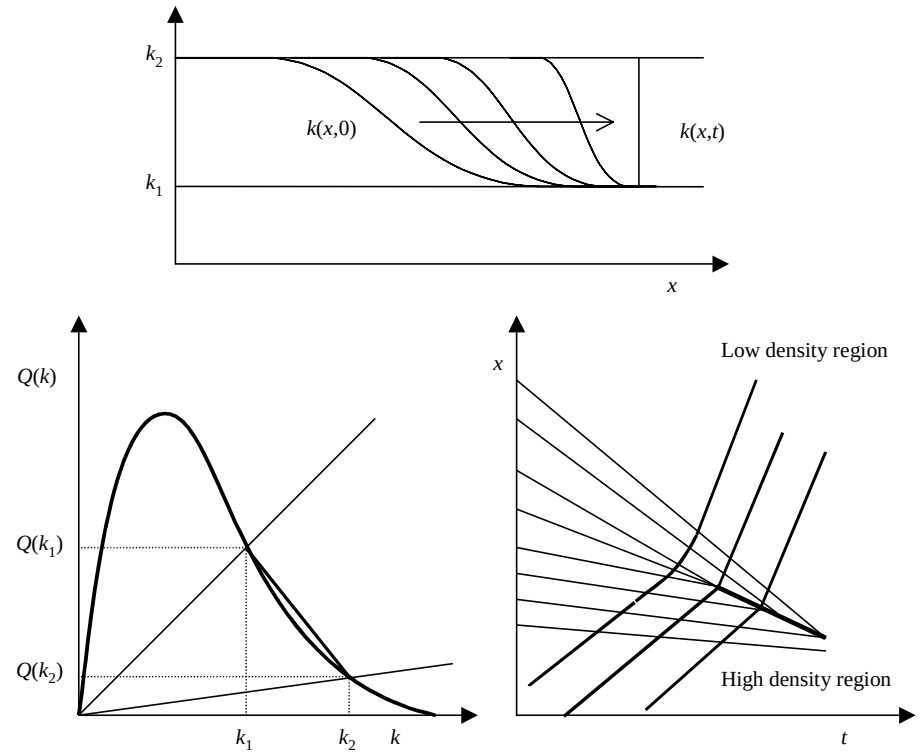

Figure 9.12: Effect of convex congested branch of $Q(k)$.

9.3 Numerical solutions to the kinematic wave model

The advantage of numerical results presented thus far is that they visually depict the effects of downstream disturbances on upstream flow. Thus they provide a good insight into the formation and dissipation of queues and congestion in time and space. The *major disadvantage* of analytical approaches is that they are generally only applicable to simple situations, e.g. cases where no on-ramps or off-ramps are present, where initial conditions and arrival patterns are simple, cases in which there is no interaction between traffic lights, etc. However, in practise, such ideal situations are seldom encountered and other approaches are needed, namely using numerical approximations.

9.3.1 Approach to numerical approximation

Numerical solution approaches come in all sizes and shapes. In most cases, however, the approaches are based on discretisation in time and space. For one, this means that the roadway is divided in small *cells* i. In most cases, these cells have a fixed length l_i (see Fig. 9.13). Cell i has interfaces at x_{i-1} and x_i, i.e. $l_i = x_i - x_{i-1}$. Furthermore, let t_j denote a discrete time instant.

Considering time instant t_j, the number of vehicles in cell i at t_j can be determined from using the cumulative flow function $\tilde{N}(x,t)$, or by integration of the density along the x. The latter yields that the number of vehicles in cell i at instant t_j equals

$$\int_{x_{i-1}}^{x_i} k\left(x, t_j\right) dx = l_i \cdot k_{i,j} \tag{9.63}$$

where $k_{i,j}$ denotes the average vehicle density (*space-averaged density*) in cell i at time instant t_j, with $T_j = t_{j+1} - t_j$. At the same time, the number of vehicles passing the interface at x_i during a period $[t_j, t_{j+1})$ can be determined directly from the cumulative flow function $\tilde{N}(x,t)$,

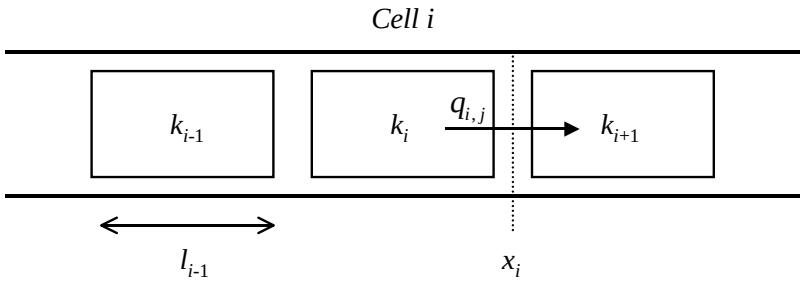

Figure 9.13: Discretisation of roadway into cells i of length l_i

or by integration of the flow rate during this period, i.e.

$$\int_{t_j}^{t_{j+1}} q(x_i, t)dt = T_j \cdot q_{i,j} \tag{9.64}$$

where $q_{i,j}$ denotes the average flow (*time-averaged flow*) across the interface at x_i during the period $[t_j, t_{j+1})$. By conservation of vehicles (or by integration of the conservation of vehicle equation (9.1) over the region $[x_{i-1}, x_i) \times [t_j, t_{j+1})$), we have

$$l_i \left(k_{i,j+1} - k_{i,j}\right) + T_j \left(q_{i,j} - q_{i-1,j}\right) = 0 \tag{9.65}$$

(assuming that the on-ramp inflows and off-ramp outflows are zero, i.e. $r = s = 0$) or

$$\frac{k_{i,j+1} - k_{i,j}}{T_j} + \frac{q_{i,j} - q_{i-1,j}}{l_i} = 0 \tag{9.66}$$

Note that the discrete representation (9.66) is still exact, i.e. no numerical approximation has been applied so far. The remaining problem is to find appropriate expressions for the time-averaged flow $q_{i,j}$. This will require two types of approximation, namely *space averaging* and *time evolution.*

9.3.2 Fluxes at cell-interfaces

In a numerical approximation scheme, in general the spaced-average densities $k_{i,j}$ are computed for all cells i and all time instants t_j. Hence, when establishing approximations for the time-averaged flow $q_{i,j}$, we need to express the flow $q_{i,j}$ as a function of the densities in the upstream cell i, the downstream cell $i+1$ at time instants t_j and t_{j+1}, i.e.

$$q_{i,j} = f\left(k_{i,j}, k_{\,i+1,j}, k_{i,j+1}, k_{i+1,j+1}\right) \tag{9.67}$$

Clearly, when the flows $q_{i,j}$ have been determined, eqn. (9.66) can be solved, either rightaway (when $q_{i,j} = f\left(k_{i,j}, k_{i+1,j}\right)$) or using an iterative approach (generally, when $q_{i,j} = f\left(k_{i,j}, k_{\,i+1,j}, k_{i,j+1}, k_{i+1,j+}\right.$ Schemes where the function f only depends on the 'current time' t_j are called *explicit schemes*; schemes where the function f depends also on the future time t_{j+1} are called *implicit schemes.* In general, explicit schemes are computationally more efficient, but less stable. For now, only explicit schemes will be considered.

9.3.3 Simple explicit schemes

The most simple scheme imaginable describes the flow $q_{i,j}$ out of cell i as a function of the conditions in that cell only, i.e.

$$q_{i,j} = f\left(k_{i,j}\right) = Q\left(k_{i,j}\right) \tag{9.68}$$

It is obvious that using this expression will not provide a realistic representation of upstream moving shock waves. Image a situation where the downstream cell $i+1$ is congested (e.g. due to a blockade upstream of the cell). The analytical solution of the kinematic model states that the flow out of cell i will be equal to zero, and that the region of jam-density will move further upstream. However, using Eq. (9.68) shows that traffic will keep flowing out of cell i. As a result, the density in the *recieving* cell $i+1$ will become unrealistically high.

An easy remedy to this problem, would be to assume that the flow out of cell $i+1$ is only a function of the conditions in the receiving cell $i+1$, i.e.

$$q_{i,j} = f\left(k_{i+1,j}\right) = Q\left(k_{i+1,j}\right) \tag{9.69}$$

Although this would clearly remedy the problem of traffic flowing into congested cells, the problem now is that the *transmitting cell* i will also transmit vehicles when its empty. Some researchers have proposed combining both approaches using weighted averages, i.e.

$$q_{i,j} = \alpha Q\left(k_{i,j}\right) + (1-\alpha)\, Q\left(k_{i+1,j}\right) \tag{9.70}$$

The problem is then to determine the correct values for α.

9.3.4 Flux-splitting schemes

A class of well-known schemes are the so-called flux-splitting schemes. Recall that the conservation of vehicle equation can be written as follows

$$\frac{\partial k}{\partial t} + c\left(k\right)\frac{\partial k}{\partial x} = 0 \tag{9.71}$$

where $c\left(k\right) = Q'\left(k\right)$. The wave speeds $c\left(k\right)$ in effect describe how information is transmitted in the flow: when $c\left(k\right) > 0$, information is transmitted downstream, i.e. from cell i to cell $i+1$. When $c\left(k\right) < 0$, the waves propagate in the upstream direction. The flux-splitting approach is aimed at splitting the flux (flow) into contributions into the downstream direction and contributions into the upstream directions. These are respectively described by

$$c^{+}\left(k\right) = \max\left\{0, c\left(k\right)\right\} = \frac{1}{2}\left(c\left(k\right) + \left|c\left(k\right)\right|\right) \tag{9.72}$$

$$c^{-}\left(k\right) = \min\left\{0, c\left(k\right)\right\} = \frac{1}{2}\left(c\left(k\right) - \left|c\left(k\right)\right|\right) \tag{9.73}$$

Note that

$$c^{+}(k) = \begin{cases} c(k) & k < k_c \\ 0 & k \geq k_c \end{cases} \quad \text{and} \quad c^{-}(k) = \begin{cases} 0 & k < k_c \\ c\left(k\right) & k \geq k_c \end{cases} \tag{9.74}$$

Note that $Q\left(k\right) = f\left(k\right) = \int c\left(\kappa\right) d\kappa$. Now, let

$$f^{\pm}\left(k\right) = \int c^{\pm}\left(\kappa\right) d\kappa \tag{9.75}$$

which in turn yields

$$f^{+}\left(k\right) = \int_0^k c^{+}\left(\kappa\right) d\kappa = \begin{cases} Q(k) & k < k_c \\ Q\left(k_c\right) & k \geq k_c \end{cases} \tag{9.76}$$

and

$$f^{-}\left(k\right) = \int_0^k c^{-}\left(\kappa\right) d\kappa = \begin{cases} 0 & k < k_c \\ Q\left(k\right) - Q\left(k_c\right) & k \geq k_c \end{cases} \tag{9.77}$$

Note that $f^{+}(k)$ is always positive, while $f^{-}\left(k\right)$ is always negative. Furthermore, note that

$$f\left(k\right) = f^{+}\left(k\right) + f^{-}\left(k\right) = Q\left(k\right) \tag{9.78}$$

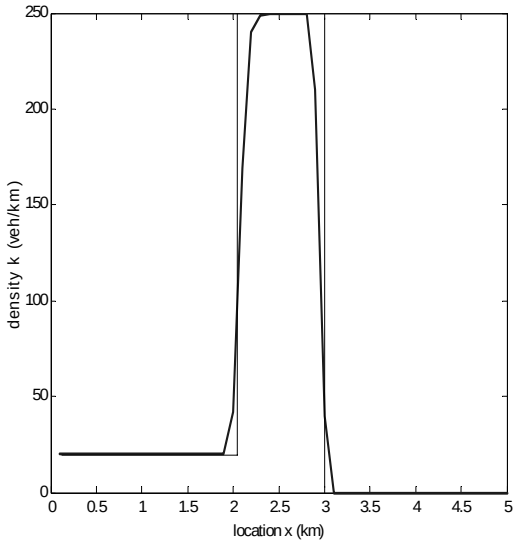

Figure 9.14: Numerical solution using flux-splitting approach and exact solution.

The flux-splitting scheme infers that the numerical flux $f^*_{i,j}$ at the cross-section x_i is approximated by considering the downstream moving contribution $f^+(k_{i,j})$ of cell i and the upstream moving contribution $f^*(k_{i+1,j})$ of cell $i+1$ as follows

$$f^*_{ij} = f^+(k_{i,j}) + f^-(k_{i+1,j}) \tag{9.79}$$

It turns out that this relatively simple scheme provides excellent results, which can be applied easily in any practical application of the kinematic wave model. From a theoretical viewpoint, the method has some undesirable properties. It is well known that the approach tends to smooth shocks. An example of this is shown in Fig. 9.14. The extent to which this occurs depends on the time-step and the cell lengths.

9.3.5 Godunov schemes

The flux-splitting approach has some practical and theoretical problems, one of which is the fact that in theory, the flux may become negative. The Godunov scheme, which closely resembles the flux-splitting scheme, does not have these drawbacks. In fact, it turns out that this scheme is both simple, and can be interpreted from the viewpoint of traffic flow theory.

Riemann problem[2]

The Godunov solution scheme is based on the solution of a specific problem, which is know as the so-called Riemann problem. The Riemann problem is defined by an intial value problem with the following starting conditions

$$u(x,0) = \begin{cases} u_L & x < 0 \\ u_R & x > 0 \end{cases} \tag{9.80}$$

Note that the LWR model assumes that the flows are in equilibrium, implying that the speeds determine the densties and the flows.

We can now define four different cases and determine the exact solution for these case. In the fist case 1, depicted by Fig. (9.15), both the downstream and upstream flow conditions

[2] In this section, we assume that the flow-density curve is concave.

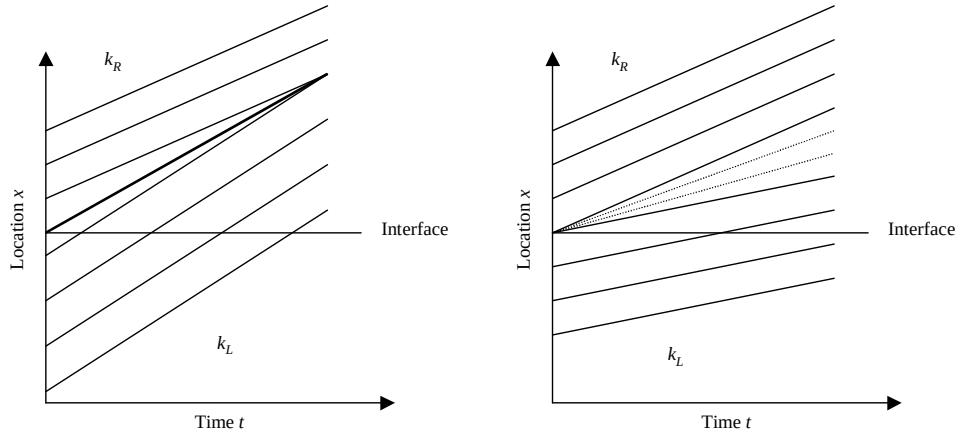

Figure 9.15: Case 1: downstream flows (k_R, u_R) and upstream flows (k_L, u_L) undercritical.

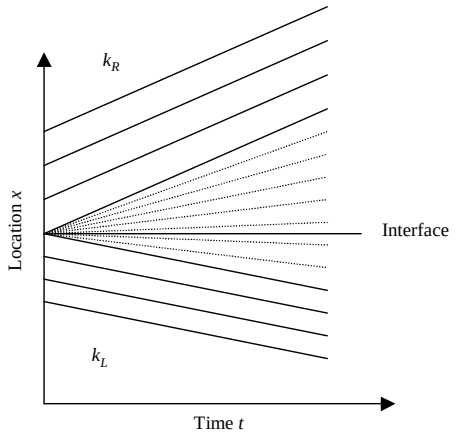

Figure 9.16: Case 2: downstream flows (k_R, u_R) undercritical and upstream flows (k_L, u_L) overcritical.

are undercritical. When $k_R > k_L$ (and thus $q_R > q_L$), an upstream moving shock wave will occur; when $k_R < k_L$, an acceleration fan will occur that describes the interface between the two regions. In either case, the flow f^* at the interface at $x = 0$ equals the downstream flow, i.e $f^* = q_L$.

Case 2 depicts the situation where the downsstream conditions k_R are undercritical, while the upstream conditions are overcritical. In this situation, shown in Fig. 9.16, an acceleration fan is transmitted from $x = 0$ at $t = 0$. Since along the interface at $x = 0$, the acceleration fan transmits a characteristic with slope 0, we can use the fact that the slope of a characteristic satisfies $c\,(k) = dQ/dk$ to see that the (constant) density along this characteristic equals the critical density k_c, and hence the flow f^* at the cross-section at $x = 0$ equals the capacity q_c.

Case 3 represents the situation where the downstream flow conditions are overcritical, while the upstream flows are undercritical. In this situation, shown in Fig. 9.17, a shock wave will emerge at $x = 0$ at time $t = 0$. The flow f^* at the cross-section at $x = 0$ depends on the direction of the shock: if the shock moves downstream, i.e. when $q_R < q_L$, the flow f^* at the interface equals the upstream flow q_L. When the shock moves upstream, which happens when $q_R > q_L$, the flow f^* at the interface equals the downstream flow q_R. Clearly, the following relation is valid in this situation: $f^* = \min\{q_L, q_R\}$.

The final case 4 (Fig. 9.18) is the case where the downstream conditions k_R and the upstream conditions k_L are overcritical. Similar to case 1, either an acceleration fan or a shock wave

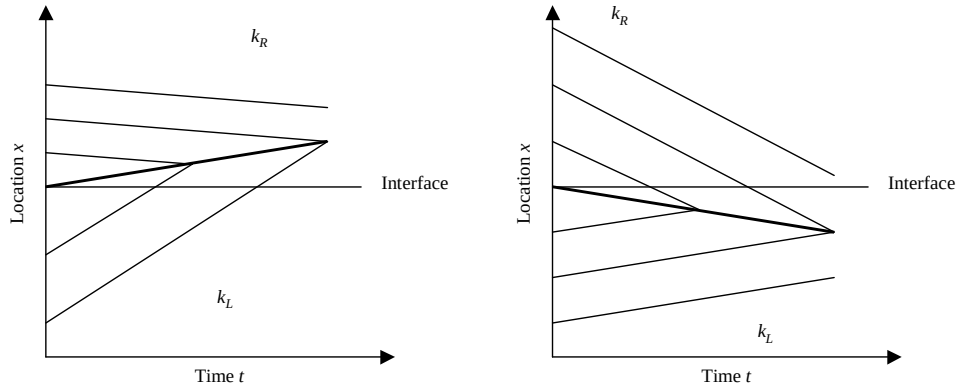

Figure 9.17: Case 2: downstream flows (k_R, u_R) overcritical and upstream flows (k_L, u_L) undercritical.

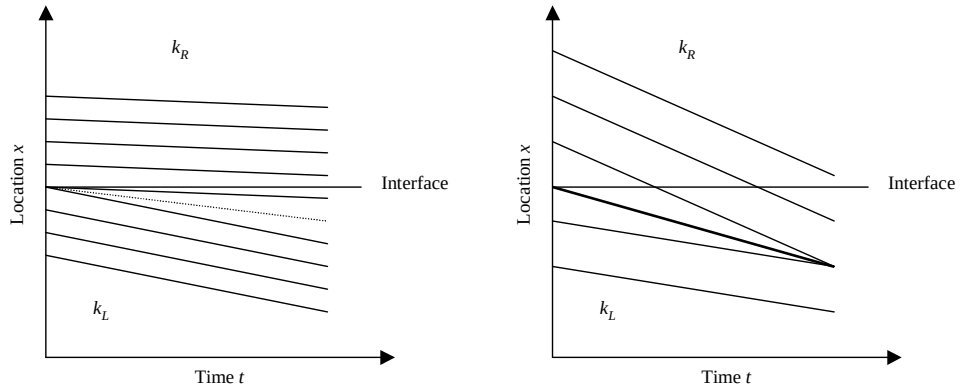

Figure 9.18: Case 4: downstream flows (k_R, u_R) and upstream flows (k_L, u_L) overcritical.

emerge. In either case, the flow f^* across the cross-section at the interface at $x = 0$ equals the flow q_R in the downstream region.

Table 9.1 summarises the results for cases 1 to 4.

Let us now defined the *traffic demand* D_L of the upstream region and the traffic supply S_R of the downstream region as follows

$$D_L = \begin{cases} q_L & k_L < k_c \\ q_c & k_L > k_c \end{cases} \tag{9.81}$$

and

$$S_R = \begin{cases} q_c & k_R < k_c \\ q_R & k_R > k_c \end{cases} \tag{9.82}$$

The traffic demand describes the traffic flow aiming to move out of the upstream region L (assuming that the flow conditions in the downstream region R allows this flow). For undercritical conditions, the demand D_L equals the flow q_L; for overcritical conditions the demand is limited to the capacity q_c.

Flow f^* at interface	$k_R < k_c$	$k_R > k_c$
$k_L < k_c$	q_L	$\min\{q_L, q_R\}$
$k_L > k_c$	q_c	q_R

Table 9.1: Flow at interface between upstream and downstream region

The traffic supply describes the maximum traffic flow the downstream region R can admit. When the conditions in the downstream region are undercritical, this flow is limited by the capacity of the road in this region; when the conditions in the downstream region are overcritical, the flow is restricted by the flow q_R in the downstream region. In a way, this flow describes the space becoming available per unit time.

Using these definitions of demand and supply, we can use the results depicted in table 9.1 to show that the realised flow f^* at the cross-section equals

$$f^* = \min\{D_L, S_R\} \tag{9.83}$$

That is, the flow f^* at the interface equals the minimum between demand and supply.

Godunov's scheme

The Godunov scheme is based on the solution to the Riemann problem. To this end, it is assumed that the conditions in the (flow) transmitting cell i and the recieving cell $i+1$ are homogeneous with the cell, i.e.

$$k(x, t_j) = k_{ij} \text{ for all } x_{i-1} \leq x \leq x_i \tag{9.84}$$

It needs no further clarification that to determine the flow at the cell interface x_i between cell i and cell $i+1$, one in fact has to solve the Riemann problem. Thus, for cell i we define the demand D_i by

$$D_i = \begin{cases} q_i = Q(k_i) & k_i < k_c \\ q_c = Q(k_c) & k_i > k_c \end{cases} \tag{9.85}$$

while for cell $i+1$ we define the supply

$$S_{i+1} = \begin{cases} q_c = Q(k_c) & k_{i+1} < k_c \\ q_{i+1} = Q(k_{i+1}) & k_{i+1} > k_c \end{cases} \tag{9.86}$$

It the time period is short enough (i.e. assuming that the conditions in cells $i-1$ and $i+2$ will not reach the interface at x_i, the flow $f^*_{i,j}$ during the period $[t_j, t_{j+1})$ equals

$$f^*_{i,j}(k_{i,j}, k_{i+1,j}) = \min\{D_i, S_{i+1}\} \tag{9.87}$$

Note that, given the assumption that the conditions in both cells i and $i+1$ are homogeneous, the flow $f^*_{i,j}$ between the cells is an exact solution of the LWR model; the approximation lies in the assumption that the homogeinity assumption holds for each time step t_j (which is obviously not true).

It turns out that the Godunov scheme has excellent properties, such as accurate representation of shocks, ability to incorporate flow-density relations that are a function of x, etc.

9.4 Higher-order models

The kinematic wave model is a simple yet sufficient theory of traffic if one only cares about the size and the end of a queue, i.e. the time-space trajectory of a shock. However, traffic flow phenomena are very complex and some rather important phenomena elude the kinematic wave model, as we have seen in chapter 5. The kinematic wave model described in the preceding chapter has been criticised by many authors, mainly because of the following reasons:

- Speeds in the kinematic wave model are described by stationary speed-concentration relations implying that the speed reacts instantaneously to the traffic concentration without any delay. Dynamic fluctuations around the equilibrium speed are observed in real-life traffic flow (hysteresis; recall the acceleration and deceleration curves from chapter 5) but are not described by the kinematic wave model.

- The kinematic wave theory shows (speed-) shock formation by steeping speed jumps to infinite sharp discontinuities in the concentration. That is, it produces discontinuous solutions irrespective of the smoothness of the initial conditions. These are in contradiction with smooth shocks observed in real-life traffic flow.
- The kinematic wave theory is not able to describe regular start-stop waves with amplitude dependent oscillation times which have been observed in real-life traffic (recall transition of synchronised flow into wide moving jams). Besides being a source of stress and irritation for drivers, stop-and-go traffic also produces higher amounts of pollutants, while leading to a higher fuel consumption due to the frequency of acceleration and deceleration.
- In real-life traffic flow, hysteresis phenomena have been observed, showing that the average headways of vehicles approaching a jam are smaller that those of vehicles flowing out of a jam (in case of relaxation dominant phase; see chapter 5). These phenomena are not described by the kinematic wave theory.
- Kinematic wave models do not address the issue of traffic instability. It has been often observed that in a certain traffic concentration range, small perturbations can induce violent transitions.We again refer to chapter 5 where the issue of traffic instability was discussed.

To resolve these problems, different approaches have been considered in the past.

9.4.1 Derivation of the model of Payne

The model of [42] consist of the conservation of vehicle equation, and a dynamic equation describing the dynamics of the speed $u(x,t)$. The model can be derived in several ways, but the most intuitive one is by considering the following, simple car-following model

$$v_\alpha(t+\tau) = \tilde{V}(s_\alpha(t)) = V\left(\frac{1}{s_\alpha(t)}\right) \tag{9.88}$$

where $s_\alpha(t) = x_{\alpha-1}(t) - x_\alpha(t)$ denotes the distance headway with between vehicles $\alpha-1$ and α. Eq. (9.88) describes how vehicle α adapts a speed $\tilde{V}$ that is a function of the distance between him and his predecessor. However, the reaction of α will not be instantaneous, but will be delayed by the reaction time τ. Let us define

$$x_\alpha(t) = x \tag{9.89}$$

and

$$v_\alpha(t) = u(x_\alpha(t), t) = u(x,t) \tag{9.90}$$

Let us first consider the left-hand-side of Eq. (9.88). We have

$$v_\alpha(t+\tau) = u(x_\alpha(t+\tau), t+\tau) \tag{9.91}$$

Since, by the theorem of Taylor, we have

$$x_\alpha(t+\tau) = x_\alpha(t) + \tau\frac{dx_\alpha}{dt} + O\left(\tau^2\right) \tag{9.92}$$

Moreover

$$\begin{aligned} u(x_\alpha(t+\tau), t+\tau) &= u\left(x_\alpha(t) + \tau\frac{dx_\alpha}{dt} + O\left(\tau^2\right), t+\tau\right) && (9.93)\\ &= u(x,t) + \tau\frac{dx_\alpha}{dt}\frac{\partial u(x,t)}{\partial x} + \tau\frac{\partial u(x,t)}{\partial t} + O\left(\tau^2\right) && (9.94)\\ &= u(x,t) + \tau u(x,t)\frac{\partial u}{\partial x} + \tau\frac{\partial u}{\partial t} + O\left(\tau^2\right) && (9.95) \end{aligned}$$

Neglecting the higher-order terms thus yields

$$v_\alpha(t+\tau) \approx u(x,t) + \tau u(x,t)\frac{\partial u}{\partial x} + \tau\frac{\partial u}{\partial t} \tag{9.96}$$

Let us now consider the right-hand-side of Eq. (9.88). First, note that the inverse of the distance headway equals the density (evaluated at the location between vehicle α and vehicle $\alpha-1$), i.e.

$$\frac{1}{s_\alpha(t)} = \frac{1}{x_{\alpha-1}(t) - x_\alpha(t)} = k\left(x_\alpha(t) + \frac{1}{2}s_\alpha(t), t\right) \tag{9.97}$$

Again, the use of Taylor's theorem yields

$$k\left(x_\alpha(t) + \frac{1}{2}\left(x_{\alpha-1}(t) - x_\alpha(t)\right), t\right) \tag{9.98}$$

$$= k\left(x_\alpha(t), t\right) + \frac{1}{2}s_\alpha(t)\frac{\partial k}{\partial x} + O\left(s_\alpha(t)^2\right) \tag{9.99}$$

$$= k(x,t) + \frac{1}{2k}\frac{\partial k}{\partial x} + O\left(\frac{1}{k^2}\right) \tag{9.100}$$

Then

$$V\left(\frac{1}{s_\alpha(t)}\right) = V\left(k\left(x_\alpha(t) + \frac{1}{2}s_\alpha(t), t\right)\right) \tag{9.101}$$

$$= V\left(k(x,t) + \frac{1}{2k}\frac{\partial k}{\partial x} + O\left(\frac{1}{k^2}\right)\right) \tag{9.102}$$

$$= V\left(k(x,t)\right) + \left(\frac{1}{2k}\frac{\partial k}{\partial x} + O\left(\frac{1}{k^2}\right)\right)\frac{dV}{dk} \tag{9.103}$$

Neglecting the higher-order terms yields

$$\tilde{V}\left(s_\alpha(t)\right) \approx V\left(k(x,t)\right) + \frac{1}{2k}\frac{dV}{dk}\frac{\partial k}{\partial x} \tag{9.104}$$

Combining Eqn. (9.96) and (9.104) yields the Payne model, describing the dynamics of the speed $u = u(x,t)$

$$u + \tau u\frac{\partial u}{\partial x} + \tau\frac{\partial u}{\partial t} = V(k) + \frac{1}{2k}\frac{dV}{dk}\frac{\partial k}{\partial x} \tag{9.105}$$

or, in the more familiar form

$$\frac{\partial u}{\partial t} + u\frac{\partial u}{\partial x} = \frac{V(k) - u}{\tau} + \frac{1}{2\tau}\frac{dV}{dk}\frac{1}{k}\frac{\partial k}{\partial x} \tag{9.106}$$

$$= \frac{V(k) - u}{\tau} - \frac{D(k)}{\tau}\frac{1}{k}\frac{\partial k}{\partial x} \tag{9.107}$$

$$= \frac{V(k) - u}{\tau} - c^2(k)\frac{1}{k}\frac{\partial k}{\partial x} \tag{9.108}$$

where $D(k) := -\frac{1}{2}\frac{dV}{dk} = \frac{1}{2}\left|\frac{dV}{dk}\right| > 0$, and where $c^2(k) = D(k)/\tau$. For reasons which will become clear later on, $c(k)$ is generally referred to as the wave speed. Furthermore, if many applications of the Payne model, the wave speed $c(k)$ is chosen constant, i.e. $c(k) = c_0$.

Let us briefly describe the different terms that are present in the Payne model, and how these terms can be interpreted from a traffic flow point-of-view:

- In hydrodynamics, the term $u\frac{\partial u}{\partial x}$ is referred to as the *transport* or *convection term*. It describes changes in the traffic speed u due to the inflow and outflow of vehicles with different speeds.

- The term $-\frac{D(k)}{k\tau}\frac{\partial k}{\partial x}$ is the *anticipation term*, since it can describe the reaction of drivers to downstream traffic conditions.
- The relaxation term $\frac{V(k)-u}{\tau}$ describes the exponential adaptation of the speed to the concentration-dependent equilibrium speed $V(k)$.

Payne [42] has shown that his model predicts instability of the traffic flow in a certain density range. This means that small disturbances in the flow can lead to the formation of a local traffic jam. This will be illustrated in the remainder. Note that a number of high-order models fall under the same model family.

9.4.2 Mathematical properties of the Payne-type models

This section discusses some of the important properties of the Payne-type models; the derivation of these properties from the model equations (B.1) and (B.2) is explained in the subsequent sections.

We have seen that the LWR model has a single family of characteristic curves, which are described by the lines $\frac{dx}{dt} = \lambda_*$, where $\lambda_* = \lambda_*(k) = \frac{dQ}{dk}$. The Payne model has *two families of characteristics* along which the properties of the flow are transported. These characteristic curves are defined by the following ordinary differential equations

$$C_+ : \frac{dx}{dt} = \lambda_1 = u + c(k) \tag{9.109}$$

$$C_- : \frac{dx}{dt} = \lambda_2 = u - c(k) \tag{9.110}$$

It was shown that for the LWR model, the density was constant (conserved) along the characteristic. This is not the case in the Payne model; in the Payne model, the dynamics of the so-called *Riemann* or *characteristic* variables $z_{1,2}$ are described. Assuming that $c(k) = c_0$, these are defined by

$$z_1 = u + c_0 \ln k \quad \text{and} \quad z_2 = u - c_0 \ln k \tag{9.111}$$

The characterstics C_+ and C_- are sometimes refered to as the *second-order waves*, whereas the waves C_* described by $\frac{dx}{dt} = \lambda_*$ are called the *first-order waves*.

It can be shown that solutions to the Payne-model are unstable, if they satisfy the following condition.

$$k\left|\frac{dV}{dk}\right| = -k\frac{dV}{dk} \geq c(k) \tag{9.112}$$

For small densities k, condition (9.112) *will generally not hold*, implying that the Payne model would predict stable traffic flow. In other words, small perturbations $\delta k(x,t)$ and $\delta u(x,t)$ will dissipate over time. This holds equally for regions in which $dV/dk = 0$. When the concentration and the rate of decrease dV/dk is large enough, the second-order models will predict that traffic flow becomes unstable. Under unstable conditions, small perturbations will grow over time and will eventually turn into a traffic jam.

For the Payne mode, we have

$$c(k) = \sqrt{\frac{1}{2\tau}\left|\frac{dV}{dk}\right|} \tag{9.113}$$

implying that traffic flow conditions are unstable when

$$k\left|\frac{dV}{dk}\right| \geq \frac{1}{2k\tau} \tag{9.114}$$

Consider, for instance, Greenshields' fundamental diagram, we get

$$\frac{dV}{dk} = -\frac{V_0}{k_j} \tag{9.115}$$

yielding that the Payne model would predict unstable traffic conditions when

$$k \geq \sqrt{\frac{1}{2\tau}\frac{k_j}{V_0}} \tag{9.116}$$

Note that the stability of the traffic conditions increase when the relaxation time τ of the flow decreases. That is, the more timely drivers react to the prevailing traffic conditions, the more stable the resulting traffic flow conditions are. For the Payne model, traffic flow conditions are always stable in case $\tau \to 0$. For details on the mathematical analysis, we refer to appendix B of these notes.

9.4.3 Numerical simulation and high-order models

Since the mathematical properties of higher-order models are still not well understood, reliable numerical analysis is also still a problem. In appendix B, we propose a numerical scheme for general high-order models. Another numerical approximation is implemented in the METANET model, which is discussed in detail in Chapter 15.

9.5 Alternative modelling approaches and generalisations

Appendix C discusses a specific type of continuum model, namely gas-kinetic models. Appendix D discusses generalisations of macroscopic models.